Evaluation of direct grafting strategies via trivalent anchoring for enabling lipid membrane and cytoskeleton staining in Expansion Microscopy

Gang Wen,[‡] Marisa Vanheusden,[‡] Aline Acke,[‡] Donato Valli, Robert K. Neely,[†] Volker Leen,[§] Johan Hofkens[*]

Department of Chemistry, KU Leuven, Leuven, Belgium

ABSTRACT: Super resolution fluorescence microscopy is a key tool in the elucidation of biological fine-structure, providing insights into the distribution and interactions of biomolecular complexes down to the nanometer scale. Expansion microscopy is a recently developed approach for achieving nanoscale resolution on a conventional microscope. Here, biological samples are embedded in an isotropically swollen hydrogel. This physical expansion of the sample allows imaging with resolutions down to the tens-of-nanometers. However, because of the requirement that fluorescent labels are covalently bound to the hydrogel, standard, small-molecule targeting of fluorophores has proven incompatible with expansion microscopy. Here, we show a chemical linking approach that enables direct, covalent grafting of a targeting molecule and fluorophore to the hydrogel in expansion microscopy. We show application of this series of molecules in the antibody-free targeting of the cell cytoskeleton and in an example of lipid membrane staining for

expansion microscopy. Furthermore, using this trivalent linker strategy, we demonstrate the benefit of introducing fluorescent labels post-expansion by visualizing an immunostaining through fluorescent oligonucleotide hybridization after expanding the polymer. Our probes allow different labelling approaches that are compatible with expansion microscopy.

KEYWORDS: expansion microscopy, trifunctional linker, lipid membranes, actin filaments, post-expansion labeling

In 2015, Boyden and coworkers introduced expansion microscopy (ExM) as an approach that enables super-resolution imaging on a standard optical microscope.[1–3] In the ExM experiment, a fixed sample is permeabilized and structures of interest are labeled using either standard immunofluorescence or, in the case of nucleic acids, fluorescence in-situ hybridization. Next, a chemical crosslinking moiety is introduced, providing the protein[4] or nucleic acid[5] structures with a functional group that is subsequently employed to graft the fluorescent labels into the polyelectrolyte polymer meshwork. This is achieved by infusing the sample with suitable monomers and polymerizing these *in situ*. This forms a swellable hydrogel throughout the sample, which can be expanded upon dialysis with water. Expansion effectively increases the distances between neighboring molecules with a linear expansion factor of ~4.5 fold, enabling anyone with access to a conventional fluorescent microscope to visualize biomolecules with an effective resolution of ~70 nm. Furthermore, the swelling in water also results in an optically-transparent matrix with preservation of the original sample geometry. Due to this intrinsic optical clearing of the sample, ExM enables imaging with high signal to noise ratio in samples that are largely impenetrable using standard optical microscopies, making it particularly well-suited for imaging

large (multicellular) 3D samples. As such, ExM has already lead to the successful imaging of brain tissue slices, [1,2,5,6] tissue sections of clinical specimens[7] and even *Drosophila* tissues.

The combination of ExM with more established super resolution techniques has also been explored, offering an additional 4-5-fold improvement in resolution with these modalities. For example, in combination with stimulated emission depletion microscopy (STED)[6] or structured illumination microscopy (SIM)[7] lateral imaging resolution of <10 nm and 30 nm, respectively, can be achieved. To this end, novel polymer formulations and 'iterative expansion microscopy' allow similar image resolution with standard optical microscopies.[8–10] Hence, the focus for improving the ExM imaging experiment is now on the development of bespoke labeling strategies which ensure a high labeling density using alternatives to antibodies, which size can impact on imaging resolution.[11] However, not all standard staining approaches used for super resolution imaging are compatible with ExM. One example of such a labeling strategy is the use of cytostatics, such as the actin-binding peptide phalloidin, as small labeling molecules for targeting the cytoskeleton.[12,13] Such small molecules can be difficult to covalently link to the gel matrix and then are washed out of the sample during the expansion process. Indeed, labeling density in ExM remains a challenge due to fluorescence signal loss during both the polymerization and digestion steps.[6,7,14–16] Many fluorophores are prone to degradation during the radical polymerization process, with some being entirely destroyed (*e.g.* cyanine dyes).[4] Moreover, as sample homogenization through digestion is crucial for isotropic expansion, fluorescent dyes can be lost due to the random nature and incomplete efficiency of the anchoring step.[17,18] This occurs when the fraction of fluorophores attached to a proteolytically-created protein fragment, that is not also crosslinked to the polymer matrix, is lost during expansion. Finally, upon expansion, the number of fluorescent labels per voxel is diluted by a factor that equals the volumetric expansion (*e.g.* $4^3 = \sim 64$ fold for the standard

ExM protocol[1]). While this intrinsic dilution of fluorescent labels cannot be prevented, dye degradation due to radical polymerization, and proteolytic removal of dyes can. To tackle these limitations and to make expansion microscopy compatible with a broader range of fluorescent reporters, we developed a trivalent linker molecule which directly, rather than indirectly, grafts reporter groups to the polymer meshwork.

Here, we demonstrate a direct grafting approach that we term TRIvalenT anchOriNg, and refer to as TRITON. TRITON enables simultaneous targeting, labelling and grafting of biomolecules, using small molecule targeting, which is not otherwise possible in expansion microscopy, with lipid membranes as a prime example. Furthermore, we evaluate the performance of our TRITON molecules for the labeling of the cytoskeleton with small molecule ligands such as phalloidin. Finally, as labels are targeted to the relevant location within the cell or tissue and permanently bound at this location throughout the polymerization, expansion and read-out steps, we provide a tool that overcomes the loss of unanchored fluorescent dyes during expansion. Furthermore, by incorporating oligonucleotide reporter barcodes in the place of fluorescent dyes, we provide a route by which targets can be labelled post-expansion with a complementary and fluorescently-tagged oligonucleotide. Such an approach avoids loss of fluorescent signal due to the gelation reaction (radical polymerization) and allows labelling with a broad range of commercially-available oligonucleotides. TRITON enables an array of biomolecular targeting and labelling approaches within single cells, which are compatible with expansion microscopy.

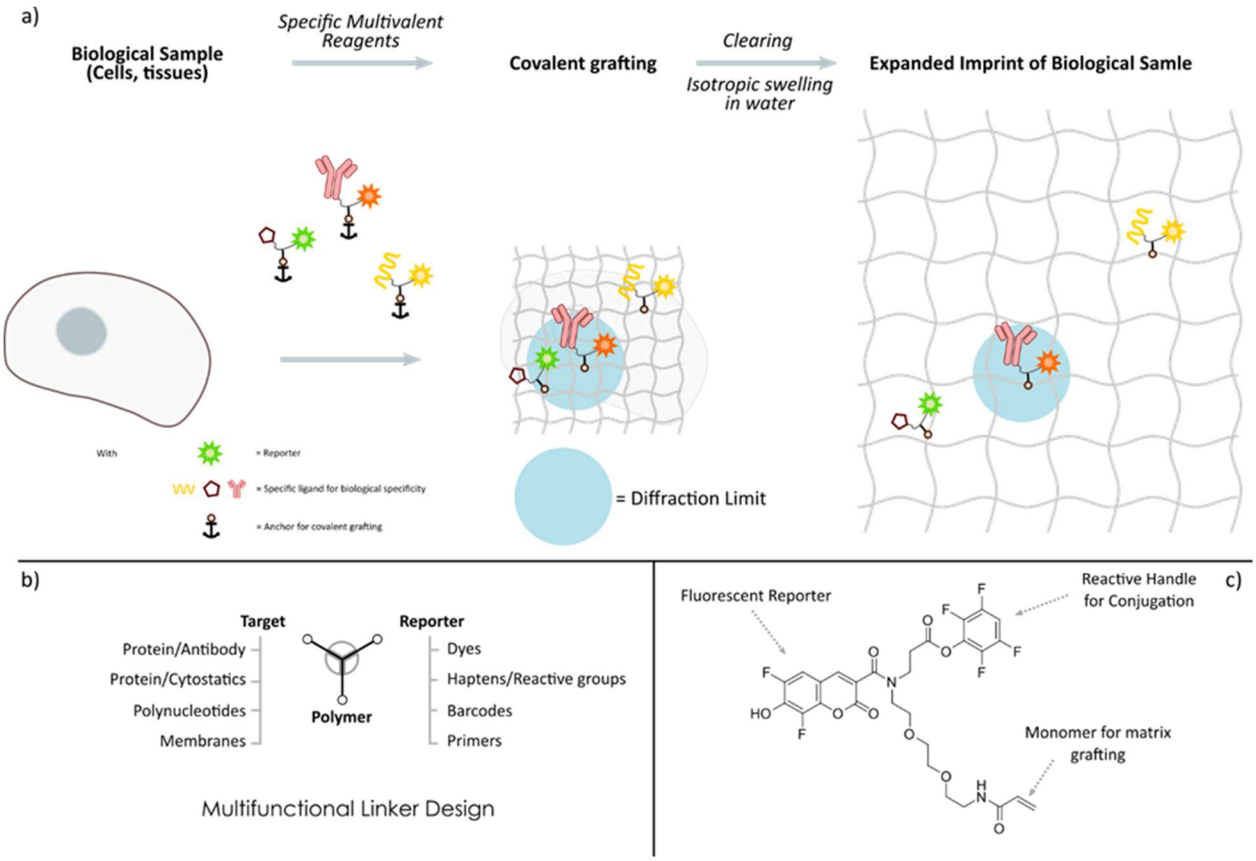

Figure 1. Image depicting the multivalent linker concept and design: a) Multivalent linkers allow for the efficient localization and grafting of signaling moieties within biological samples. b) Through flexible linker design, a range of targeting and reporting moieties can be directly conjugated to the polymer. c) Example of a TRITON trivalent linker with a fluorescent reporter (Pacific Blue), reactive tetrafluorophenyl (TFP) ester for amine conjugation and acrylamide monomer for grafting to the expansion microscopy polymer.

RESULTS AND DISCUSSION

We have developed a range of multifunctional ligands, attached to a reporter moiety in a covalent fashion through a dedicated linker. To further ensure covalent attachment of the reporter to the polymeric matrix at the location of the biological target, a monomer unit (acryloyl) is added to the structure, yielding a trifunctional linker (Figure 1).

In its most simple variant, the reporter moiety is a fluorescent dye. Here, the use of dyes with chromophores which are inert towards the radical polymerization reaction is imperative. To evaluate dye stability for use in our TRITON linkers, we screened a large library of commercial and non-commercial organic dyes for stability in the radical polymerization mixture, as measured through fluorescence intensity reduction after polymerization. The assay results are largely in line with earlier observations of Boyden *et al.* on antibody coupled organic fluorophores (SI),[4] where chemical robustness of the chromophore against radical reactions is key to signal survival.

Based on the outcome of these results, a portfolio of the best performing fluorescent dyes in ExM were prepared as trivalent compounds, linked to a targeting group and a acryloyl-moiety (anchor). We evaluated these for direct fluorescent labeling of cellular structures through coupling to a range of selected targeting groups (General structure, Figure 1, panel C, full structures in SI).

Small-molecule targeting of tri-functional labels

As cytoskeletal labeling is both of high biological relevance and often used for evaluating performance in different super resolution approaches, these compounds provided the proving grounds for the TRITON approach. However, labelling of actin has not previously been reported in expansion microscopy because the phalloidin conjugates, typically used for targeting actin cannot be readily functionalized to carry both a fluorophore and an anchoring (acryloyl) moiety. Hence, we prepared a set of fluorescent TRITON compounds that couple a range of cytostatic moieties to fluorophores and anchors. For actin staining, a set of phalloidin conjugates were prepared in a single step from a multivalent linker backbone, with fluorescent reporter dyes spanning the visible spectrum (full structures and synthetic procedure in SI). In cellular experiments, the TRITON phalloidin conjugate will efficiently stain the cytoskeletal actin (Figure

2, panel a-f) in pre-expansion images following standard protocols, and upon expansion. Some sample drift was experienced during post-expansion imaging, an issue that is well known in expansion microscopy. From the different sample mounting approaches that are reported in literature,[19] we immobilized expanded specimens by re-embedding them in a charge-neutral polyacrylamide gel, an approach which would also be compatible with the dark oligonucleotide labels described further in the manuscript. As a consequence of this measurement, the gel shrinks around 30% in size and fluorescent dyes are partially more degraded due to the second radical polymerization step.[5] By comparing the same nuclear area in the pre- and post-expanded image, we calculated a linear expansion factor of ~3.2x, which gives a theoretical resolution for the expanded sample of 114 nm based on the Rayleigh criterion. This is consistent with measurements of the full width at half maximum (FWHM) illustrating an effective resolution of ~125 nm is achieved after expansion (line profiles were selected for the pre- and post-expansion images and are indicated in figure 2c and f, corresponding intensity plots and Gaussian fits on raw data in SI, Figure S4). These numbers clearly show our TRITON molecules are indeed suitable probes for expansion microscopy since they are matching theoretical expectations.

Another upcoming field in SR microscopy is the study of membrane structures, mostly composed of lipids and proteins. Although protein structures can easily be visualized with nanoscale resolution through expansion microscopy, lipids cannot. Nevertheless, studying membrane structures could really benefit from expansion microscopy due to the asymmetry between the inner and outer leaflet of different membranes,[20] and the small size of intracellular membranous structures.[21] Also, membrane folding like the inward or outward budding of microvesciles could be an interesting biological event to further investigate since recent studies state these vesicles play not only an important role in the extracellular communication and progression of cancer cells but

also stimulate multiple drug resistance pathways [22,23], so it could be of great interest to study these type of structures with preserved spatial information in high resolution. Where other super resolution approaches require dyes with unique specifications and are thus difficult to combine with the limited repertoire of fluorescent membrane probes, with the exception of the membrane-binding fluorophore-cysteine-lysine-palmitoyl group (mCLING),[24] expansion microscopy is less dependent on this. As most fixations use aldehydes to form chemical cross-links between reactive lysine groups, and as most lipids or their membrane probes are not strongly reactive with aldehydes, they remain mobile after chemical fixation. Upon permeabilization, digestion and expansion, the majority of lipids will be solubilized and washed out of the expandable polymer, which is the main reason for being incompatible with ExM. We reasoned that a TRITON molecule could provide a potential solution, and, in what is an example of lipid membrane expansion microscopy, trivalent fluorescent lipids, carrying DSPE (1,2-Distearoyl-sn-glycero-3-phosphoethanolamine), stain phospholipid bilayers, with the membrane structure and microstructure clearly visible after the expansion process. (Figure 2, panel g-l, structure in SI). More specifically, both the plasma membrane and nuclear envelope can clearly be distinguished from each other but also several organelle structures and different vesicles inside the cellular environment start to become noticeable after expansion.

Upon examination of the image panels displaying the lipid membrane staining, it should be noted that the areas shown pre- and post-expansion appear to be not completely identical. We attribute this to a mismatch in the z-plane that was recorded in these two cases (a video of pre- and post-expansion Z-stack is included in the Supporting Information). To avoid drift during imaging of the expanded sample, all excess of water was removed. However, sample mounting by re-embedding was not applied to prevent further dye degradation such as was experienced during the phalloidin

experiment. Nevertheless, shrinking of the gel over time was unavoidable since water will gradually start leaking out of the sample if it is no longer in solution. An expansion factor of ~3.3x was calculated for this sample after measuring the same nuclear area pre and post expansion. Based on this analysis, the theoretical resolution of the image is approximately 70 nm after expansion which again matches measurements of the full width at half maximum (FWHM) in both the nuclear and plasma membrane showing on average an apparent resolution of ~76nm post expansion (line profiles were selected for the pre- and post-expansion images and are displayed in figure 2i and l, corresponding intensity plots and Gaussian fits on raw data in SI, Figure S5).

This experiment is also a testimony to the overarching concept of substituting a biological structure with permanently-tethered labels, as lipid membranes structures will not survive the expansion process, but their signal is permanently imprinted using our TRITON approach.

In general, the fluorescent TRITON tags provide excellent staining of their biological targets, with signals retained after swelling, across a range of fluorophore excitation/emission wavelengths. This establishes a general method for providing permanent signatures of biomolecular fine structures, with the possibility of directly generating constructs for various targets, with a minimal number of preparative steps.

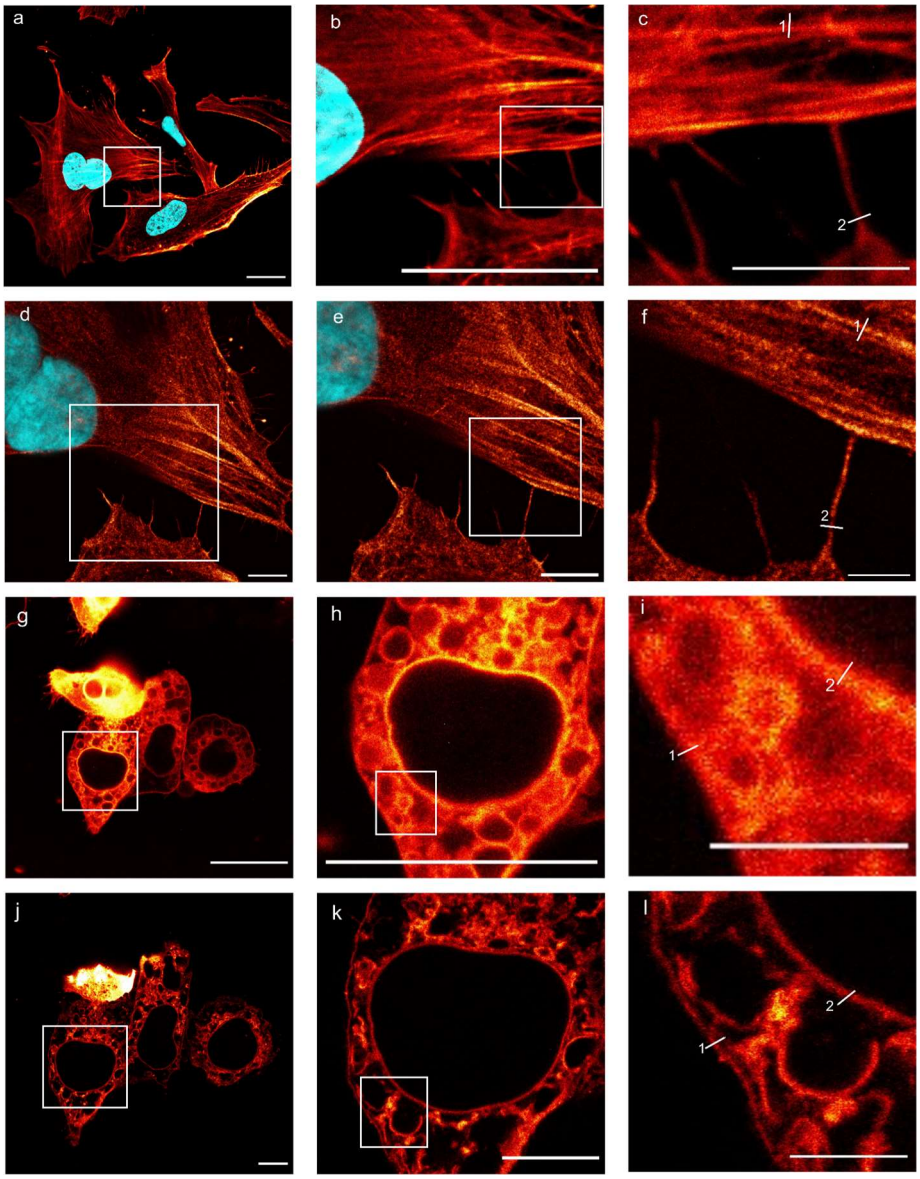

Figure 2. TRITON labels applied in ExM across a range of biological targets: a-f) Direct cytoskeleton staining (actin) through a fluorescent phalloidin trivalent linker (Rhodamine B, phalloidin, pre- and post-expansion). **(a)** pre-expansion image obtained by 63x objective (NA 1.2) with zoom **(b, c)** of the boxed area and a measurement of the FWHM indicated by line profiles (1) 400 nm and (2) 260 nm, **(d)** post-expansion image obtained by 25x objective (NA 0.95) with zoom in **(e, f)** and FWHM line profiles (1) 140 nm and (2) 110 nm. g-l) Expansion of cellular phospholipid membranes through lipid conjugation to a fluorescent trivalent linker (Pacific Blue,

DSPE, pre- and post-expansion). **(g)** pre-expansion image obtained by 63x objective (NA 1.2) with zoom **(h, i)** of the boxed area and FWHM line profiles (1) 260 nm and (2) 320 nm , **(j)** post-expansion image obtained by 63x objective (NA 1.2) with zoom in **(k, l)** and line profiles for FWHM measurements (1) 82 nm and (2) 70 nm. Scale bars: 25 µm (a, b, d, e, g, h, j, k); 10 µm (c, f, l); 5 µm (i)

Immunostaining using tri-functional labels

As discussed above, the reaction conditions of the polymerization process lead to moderate to near-complete destruction of many fluorescent dyes. To circumvent this issue, bio-orthogonal reactive groups and/or haptens can be grafted onto the polymer matrix, as "dark" labels prior to polymerization. After the polymerization, these dark labels can be bound by a partner carrying the read-out signal, *e.g.* reactive dyes or fluorescent proteins. Such an approach can be employed either before or after expansion of the hydrogel. The potential of such a post-polymerization labeling step and its impact on brightness in ExM is exemplified by a recent manuscript of Shi and coworkers.[25] In a further example, we demonstrate the application of DNA oligonucleotides as a docking strand for a fluorescently tagged reporter oligo, which can be readily combined with the multifunctional TRITON linkers. After labeling the cellular target- the trivalent structure carrying the DNA docking strand- is covalently anchored in the polymeric matrix, leaving a encoded, targetable group for a specific biological structure in the post-ExM sample.

DNA oligonucleotides (OD) are attached to the TRITON linker through active ester-based coupling with amine terminated oligonucleotides or thiol-maleimide chemistry. These stable conjugates can be directly coupled to *e.g.* antibodies in a single step reaction. Consistent with previous examples of the staining of a range of biomolecules in expanded gels, we were able to

use OD-labeled antibodies (Figure 3) for specific recognition of their respective targets, followed by gelation, expansion and hybridization with fluorescently labeled reporter probes. As such, we effected immunostaining of alpha-tubulin via direct grafting of DNA-conjugated secondary antibody and fluorescent oligo-based readout post-expansion. This is a further example of how the addition of fluorescent dyes post-expansion allows use of *e.g.* cyanine reporter dyes in ExM, a dye otherwise destroyed in the polymerization process. It should also be noted that this method allows for highly multiplexed imaging, without being inherently restricted to the spectrally resolvable dyes. In addition, this approach allows an assessment of the impact of the labeling scheme, and while rhodamine B direct staining is quite resistant to radical polymerization, post-expansion labeling through a fluorescent readout oligo clearly performs better, likely due to signal loss of the rhodamine B during polymerization (survival rate approx. 50-60%, SI, Graph S1). These examples demonstrate that the use of oligo-reporters in combination with the use of primary antibodies has significant potential for multiplexed imaging, in ExM, where a high signal-to-noise ratio in the image is desirable.

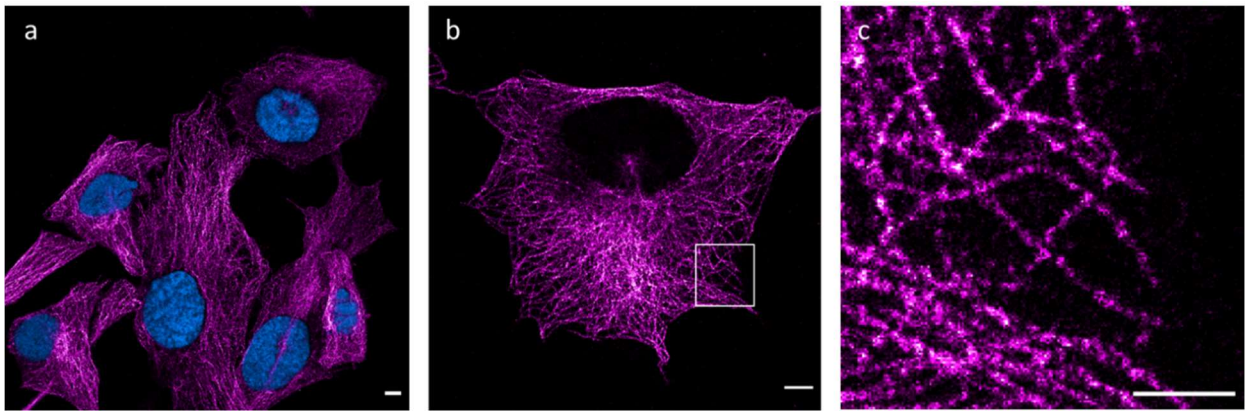

Figure 3. Immunostaining of alpha-tubulin via direct grafting of DNA-conjugated secondary antibody and fluorescent oligo-based readout post-expansion. (a) Two-color image with a nuclear DAPI staining in cyan and immunostaining of alpha-tubulin, visualized with readout oligo (Cy5,

sequence in SI) in magenta. (b) same staining as (a), with the DAPI-channel removed to show the high signal to noise ratio and low background staining in the nucleus. (c) Zoom of the boxed area in (b). Scale bars: 10 μm (a-b), 5 μm (c).

CONCLUSIONS

We describe the concept of TRITON labels for application in expansion microscopy. These molecules represent a set of trifunctional compounds that allow the direct grafting of a fluorophore, targeted to a epitope of interest to the hydrogel network used for expansion. We have shown how these compounds can be adapted for imaging of a range of biological targets and across a range of wavelengths. We demonstrated several methods for targeting of fluorophores using TRITON; by direct conjugation to a small molecule and by conjugation to an antibody for post-gelation oligonucleotide hybridization. By doing so, we demonstrate targeting of actin and lipid membranes in expansion microscopy. Furthermore, post-gelation labelling with fluorescently-tagged oligonucleotides will enable complex, multiplexed imaging experiments in ExM, in the future. TRITON enables fluorescent labelling using small molecules in ExM, is simple to apply with standard immunolabelling and will allow massively multiplexed readout in ExM, in the future.

METHODS

Materials

Unless otherwise indicated, all solvents and organic reagents were obtained from commercially available sources and were used without further purification. Dry solvents for reaction were used as received from commercial sources.

Characterization

All reaction progress was monitored using thin layer chromatography (TLC) with silica gel plates (Kieselgel 60 F254 plates, Merck) under UV light and LC-MS (Waters Acquity UPLC/ SQD). Mass spectra was obtained using a Waters Acquity UPLC-SQD mass spectrometer. ^{1}H NMR spectra was recorded on a Bruker Avance 300 MHz, 400 MHz or a Bruker Avance II+ 600 MHz instrument, and ^{13}C NMR spectra was recorded at a Bruker 600 Avance II+ instrument using DMSO-d_6, MeOD-d_4 or $CDCl_3$ as a solvent and tetramethylsilane (TMS) as an internal standard.

Synthesis of TRITON linker

Synthesis of tert-butyl (2-(2-(2-aminoethoxy)ethoxy)ethyl)carbamate

To a solution of 1,2-bis(2-aminoethoxy)ethane (13.1 mL, 89.7 mmol) in dry DCM (80 mL) was added a solution of di-tert-butyl dicarbonate (2.91 g, 15.0 mmol) in dry DCM (25 mL) dropwise at 0 ºC over 30 min. The reaction mixture was allowed to warm to room temperature and stirred overnight at the same temperature. After the reaction finished, the solvent was removed under reduced pressure. The residue was dissolved in water (30 mL) and then extracted with DCM (35 mL, 4x). The combined organic phase was dried over $MgSO_4$ and evaporated to get the intermediate **S1** as a light yellow oil (86%).

Synthesis of tert-butyl 2,2-dimethyl-4-oxo-3,8,11-trioxa-5,14-diazaheptadecan-17-oate

To a solution of tert-butyl (2-(2-(2-aminoethoxy)ethoxy)ethyl)carbamate (4.3 g, 17.4 mmol) in EtOH (50 mL) was added tert-butyl acrylate (2.25 g, 17.6 mmol) and triethylamine (2.4 mL, 17.4 mmol), the reaction mixture was stirred overnight at room temperature. After complete reaction, the solvent was removed under reduced pressure and the residue was purified by column chromatography to obtain the desired product **S2** as a light yellow oil (58%).

Synthesis of N-(9-(2-((2-(2-(2-ammonioethoxy)ethoxy)ethyl)(2-carboxyethyl)carbamoyl)phenyl)-6-(diethylamino)-3H-xanthen-3-ylidene)-N-ethylethanaminium

To a solution of Rhodamine B (1 g, 2.09 mmol) in DMF (10 mL) was added triethylamine (0.87 mL, 6.27 mmol) and HBTU (0.87 g, 2.30 mmol). After 10 minutes, **S2** (0.87 g, 2.30 mmol was added and the reaction mixture was stirred at room temperature for 2 h. After complete reaction, 50 mL ethyl acetate was added into the reaction flask, followed by washing with water (50 ml, 2 x) and brine (50 mL). The organic layer was dried over $MgSO_4$ and evaporated to get the intermediate **S3**, of sufficient purity for further use.

To a solution of the intermediate **S3** in DCM (2 mL) was added TFA (2 mL) and the reaction mixture was stirred overnight at room temperature. After the reaction finished, evaporated all solvents to get the product **S4** as a red solid (60%).

Synthesis of N-(9-(2-((2-(2-(2-acrylamidoethoxy)ethoxy)ethyl)(2-carboxyethyl)carbamoyl)phenyl)-6-(diethylamino)-3H-xanthen-3-ylidene)-N-ethylethanaminium

To a solution of the intermediate **S4** (0.757 g, 1.11 mmol) in MeOH: THF (v:v = 2 mL: 3 mL) was added a solution of Na_2CO_3 (0.239 g, 2.25 mmol) in water (3.5 mL) under the protection of N_2, followed by cooling the reaction flask to 0°C with an ice bath. A solution of acryloyl chloride (90 μL, 1.11 mmol) in dry dioxane (0.55 mL) was added dropwise to the reaction flask, and the reaction mixture was allowed to come to room temperature over 20 min. After complete reaction, all solvents were evaporated and the residue was purified by column chromatography to yield the product **S5** as a red solid (40%).

Synthesis of N-(9-(2-((2-(2-(2-acrylamidoethoxy)ethoxy)ethyl)(3-oxo-3-(2,3,5,6-tetrafluorophenoxy)propyl)carbamoyl)phenyl)-6-(diethylamino)-3H-xanthen-3-ylidene)-N-ethylethanaminium

To a solution of the intermediate (0.50 g, 0.68 mmol) in ACN (3 mL) was added DCC (0.14 g, 0.71 mmol) and 2,3,5,6-Tetrafluorophenol (0.118 g, 0.71 mmol), successively. The reaction was stirred at room temperature under the protection of N_2 for 2 h. After the reaction finished, the solution was filtered to remove filtration. Then, the solvent was removed under reduced pressure and the residue was purified by column chromatography to yield the product **S6** as a red solid (25%).

Synthesis of small-molecule multifunctional linkers: Rh B-Phalloidin Linker

To a solution of the active ester intermediate Rhodamine B conjugated with TFP and acryloyl amide (0.1 μmol) (General procedure 1) in DMSO (20 microliter) was added phalloidin amine (tosylate) one equivalent, as 2 mM solution in DMF), and the resulting reaction mixture was stirred at 30 ^{o}C for 2h. Upon indication of complete reaction, the crude mixture was purified using preparative HPLC [Shim-pack GIST C18 2 μm column, Eluent A: 0.1% HCOOH in Milli-Q water, Eluent B: MeOH, gradient elution (20%-100% B from 0-30 min; 100% B from 30-35 min), pump flow: 2.00 mL/min, T_R = 18.94 min], and the desired products **S7** was used as such.

Other analogues were synthesized and purified based on the same method as described above, just using different dyes.

Synthesis of 2-(2-(2-(N-(2-carboxyethyl)-3-(2,5-dioxo-2,5-dihydro-1H-pyrrol-1-yl)propanamido)ethoxy)ethoxy)ethan-1-aminium

To a solution of Succinimidyl 3-maleimidopropionate (0.32 g, 1.20 mmol) in DMF (4 mL) was added triethylamine (0.35 mL, 2.50 mmol) and **S2**. The reaction mixture was stirred at room temperature for 2 h. After complete reaction, 50 mL ethyl acetate was added into the reaction flask, followed by washing with water (50 mL, 2 x) and brine (50 mL). The organic layer was dried over $MgSO_4$ and evaporated to get the intermediate without further purification. To a solution of the intermediate in DCM (2 mL) was added TFA (2 mL) and the reaction mixture was stirred overnight at room temperature. After the reaction finished, evaporated all solvents to obtain the product **S8** as a light yellow oil (90%).

Synthesis of 4-(3-(2,5-dioxo-2,5-dihydro-1H-pyrrol-1-yl)propanoyl)-14-oxo-7,10-dioxa-4,13-diazahexadec-15-enoic acid

To a solution of the intermediate **S8** (0.458 g, 0.94 mmol) in MeOH: THF (v/v 2:3, 5 mL) was added a solution of Na_2CO_3 (0.200 g, 1.89 mmol) in water (3.5 mL) under the protection of N_2, followed by cooling the reaction flask to 0°C with an ice bath. A solution of acryloyl chloride (99 µL, 1.23 mmol) in dry dioxane (0.85 mL) was added dropwise to the reaction flask, and the reaction mixture was allowed to come to room temperature over 20 min. After complete reaction, all solvents were evaporated and the residue was purified by column chromatography to obtain the desired product **S9** as a clear white oil (70%).

Synthesis of 2,3,5,6-tetrafluorophenyl 4-(3-(2,5-dioxo-2,5-dihydro-1H-pyrrol-1-yl)propanoyl)-14-oxo-7,10-dioxa-4,13-diazahexadec-15-enoate

To a solution of the crude reaction intermediate (0.40 g, 0.95 mmol) in ACN (5 mL) was added DCC (0.233 g, 1.14 mmol) and 2,3,5,6-Tetrafluorophenol (0.189 g, 1.14 mmol), successively. The reaction was stirred at room temperature under the protection of N_2 for 2 h. After the reaction

finished, the solution was filtered to remove filtration. Then, the solvent was removed under reduced pressure and the residue was purified by column chromatography to obtain the desired product **S10** as a clear white oil (30%).

Synthesis of small-molecule multifunctional linkers: Pacific Blue-lipid Linker

To a solution of the active ester intermediate Pacific blue conjugated with TFP and acryloyl amide (14 mg, 0.022 mmol) (General procedure 1) in Chloroform: water (v:v, 5:1, 6 mL) was added triethylamine (6 μL, 0.043 mmol) and 1,2-Distearoyl-sn-glycero-3-phosphoethanolamine (17.8 mg, 0.024 mmol), and then the resulting reaction mixture was stirred overnight at room temperature. Upon indication of complete reaction, the crude mixture was purified by column chromatography, and the desired products **S11** was obtained as a pale yellow film.

Cell culture

HeLa cells (ATCC) and HeLaP4 cells (a kind gift of the institute of Molecular Virology and Gene therapy, KULeuven) were cultured at 37 °C in a 5 % CO2 humidified atmosphere in high glucose (4.5 g/L), glutamine free, phenol red-free Dulbecco's Modified Eagle Medium (DMEM; Life Technologies) supplemented with 10% (v/v) fetal bovine serum, 50 μg/mL gentamicin (Life technologies) and 1% glutamax. When cells reached 70 % confluency, they were washed with 1x DPBS (no calcium, no magnesium; Life Technologies) before detaching with 10x TrypLETM Enzyme (Life Technologies). Afterwards, cells were seeded into the correct imaging chambers depending on the experiment.

Cytostatics

HeLa cells were seeded into 8-well chambers (Thermo Scientific, 155411) at a density of 25 x 10^3 cells/well. The next day, cells were fixed in 4% paraformaldehyde (PFA) for 10 minutes and washed 3x for 5 minutes with 1x PBS before permeabilization with 0.2% Triton X-100 at room temperature for 15 minutes. Cells were then washed with 1xPBS followed by at least 1h incubation with 0.25 µM of a multivalent linker with phalloidin-Rhodamine B targetting F-actin. After staining, all cells were washed for 5 minutes with 1x PBS before imaging.

Immunostaining

HeLa cells were seeded onto size 22 mm x 22 mm #1.5 coverglasses at a density of 40 x 10^3 cells/cm^2 and cultured as mentioned in the previous section. The next morning, cells were fixed in 4% PFA for 10 minutes and PFA was quenched in NH_4Cl for 10 minutes. Cells were permeabilized with 0.2% Triton X-100 for 15 minutes at room temperature, washed 3x for 5 minutes with 1x PBS and blocked with blocking buffer (10% fetal bovine and 0.1% Tween-20 in 1x PBS) for 15 minutes. Next, coverslips were incubated with primary antibodies (mouse anti α-tubulin, Abcam, ab7291) in blocking buffer at a concentration of 2 µg/mL for 1 hour at room temperature and washed with PBS three times for 5 minutes each. Specimens were incubated with DNA-conjugated antibodies (Donkey Anti-Mouse IgG, Abcam ab6707) for 1 hour in blocking buffer at a concentration of 10 µg/mL or with a dilution of 1:100, respectively, and washed with blocking buffer three times for 5 minutes each.

Lipid staining

HeLaP4 cells were cultured into 8-well chambers (Thermo Scientific, 155411) at a density of 25 x 10^3 cells/well. After 24 hours, cells were fixed in 4% PFA for 10 minutes and washed with 1xPBS before permeabilization with 0.5% Tween-20 at room temperature for 10 minutes. After washing the cells 3 times for 5 minutes with 1x PBS, membranes were stained for 1 h with 50 µM trivalent lipids followed by washing for 5 minutes with 1x PBS before imaging.

Gelation, digestion, expansion and post-expansion labeling

Gelation solution (1 x PBS, 2 M NaCl, 8.625% (w/w) sodium acrylate, 2.5% (w/w) acrylamide and 0.15% (w/w) N,N'-methylenebisacrylamide enriched with 0.15% tetramethylenediamine, 0.15% ammonium persulfate and 0.01% 4-hydroxy-TEMPO) was prepared and kept on ice until further use to prevent premature gelation. A gelation chamber was prepared by placing two size 22 mm x 22 mm #1.5 coverslips on a Sigmacote® (Sigma Aldrich) treated glass slide spaced by ± 1.5 cm. Next, cells were washed with the gelation solution, gelation solution was removed again and a 80 µl droplet of gelation solution was placed in between the two size 22 mm x 22 mm #1.5 coverslips. The coverslip containing the sample was then introduced on top of the gelation chamber, cells facing down, and the construction was sealed using 4 binder clips. Gelation took place at 37 °C under N_2 atmosphere for 2 hours. After gelation, the Sigmacote® treated glass slide was carefully removed from the gelation chamber using the sharp edge of a razor blade and using the same razor blades, the desired size of the gel was cut out. Gels were transferred to a 6-well plate, making use of the supporting coverslip, and incubated in 2-3 mL of proteinase K (New England Biolabs) diluted to 8 U/mL in digestion buffer (50 mM Tris (pH 8), 1 mM EDTA, 0.5% TritonX-100, 0.8 M guanidine HCl) for 12 h at RT. Fluorescently stained samples were expanded

by incubation in an excess of deionized water 4 times for 10 minutes each. Samples stained with DNA-conjugated antibodies were washed 3 times for 30 minutes each with PBS, incubated in hybridization wash buffer (20% formamide in 2x SSC) for 10 minutes and incubated overnight with 100 nM readout oligo in hybridization buffer (20% formamide, 10% dextran sulfate, 0.1% Tween-20 in 2x SSC) in an airtight container at 37°C. After hybridization, gels were washed 1 time for 10 minutes with hybridization wash buffer supplied with 1 µg/mL DAPI and two times for 10 minutes each with hybridization wash buffer. Finally, gels were expanded with 0.5x PBS.

Re-embedding of expanded gels in acrylamide matrix

For phalloidin staining, re-embedding expanded gels in a charge-neutral polyacrylamide gel is an option to reduce the hydrogel drift. After samples were incubated in 2-3 mL of proteinase K (New England Biolabs) diluted to 8 U/mL in digestion buffer (50 mM Tris (pH 8), 1 mM EDTA, 0.5% TritonX-100, 0.8 M guanidine HCl) for 12 h at RT, gels were transferred to a bind-silane treated well (Bind-silane solution: 4 mL ethanol, 100 µL acidic acid, 5 µL bind-silane, 900 µL MQ) and expanded with deionized water 4 times, 20 min each time. After that, expanded gels were washed by re-embedding solution (1 mL 5 mM tris pH 10.5, 600 µL 3 % acrylamide, 750 µL 0.15% N,N'-methylenebisacrylamide, 7.75 mL deionized water) one time and then incubated in re-embeding solution in fridge for 20 minutes. Finally, the solution was removed and incubated at 37 °C for 2 hours in a nitrogen-filled chamber.

Fluorescence imaging

Imaging was performed on an inverted Leica true confocal scanner SP8 X system (Wetzlar, Germany) equipped with a HCPLAPO CS2 63X water immersion objective (NA 1.2) or Fluotar VISIR 25X water immersion objective (NA 0.95). DAPI stainings were imaged using a 405 nm

pulsed diode laser. A supercontinuum white light laser (SuperK EXTREME/FIANIUM, NKT photonics, Birkerød, Denmark) was used for the excitation of all other fluorophores and laser light was filtered by a notch filter when the correct wavelength was available. Prism dispersion and spectral detection were used to separate the correct signal picked up by a Leica Hybrid Detector. The laser power of the supercontinuum white light laser, the gain, the pinhole size (1 airy unit (AU)) and the line averaging were kept constant when samples were compared. Occasionally 0.3 - 12.0 ns gating was applied to minimize reflection when imaging close to the coverslip. Leica Application Suite X was used to acquire the images which were post-processed using ImageJ and Huygens Professional (Scientific Volume Imaging b.v.). All images were collected using Nyquist sampling theorem.

It should be noted that, in line with fluorophore dilution in expansion, the strong decrease of fluorescence intensity per volume in expansion can make the use of high laser power (*e.g.* 100-fold increase 1.84 µW to 188 µW) unavoidable in certain cases.

Antibody-Oligo Conjugates

Antibody-Oligo conjugates were prepared using standard procedures (See Hermanson, Bioconjugate Techniques). For example, encoding oligo (NH2 terminated, 2 mM in PBS (pH 7.2), 50 µL, 100 nmol)) was reacted with S8 (10 equivs, as a DMSO solution) by incubating at 37 °C for 60 minutes. After complete reaction, the DNA was purified through ethanol precipitation (See above). The dried DNA pellet is resuspended in 1x PBS (pH 7.2) and stored at -20°C. Simultaneously, the desired antibody is reacted with 2-iminothiolane (5-20 equivalents, 60 minutes at RT) and after reaction the antibody was purified in 1x PBS using 0.5 ml 40 kDa Zeba desalting columns (ThermoFisher #87766). The activated antibody is combined with the

functionalized oligo in the desired ratio (*e.g.* 1:40) and reacted for 60 minutes at room temperature, followed by purification and concentration using Amicon Ultra 0.5 mL 50 kDa Centrifugal Filters (EMD Millipore #UFC510096). The functionalized antibodies are stored at 4°C. Validation of oligo-antibody conjugation was conducted through denaturing SDS-PAGE gel assay by denaturing antibodies in LDS sample buffer (ThermoFisher #NP0007) with reducing agent (50 mM DTT) at 70 °C for 10 minutes. Next, samples were run on a NuPage 4-12% Bis-Tris PAGE gel (ThermoFisher #NP0322PK2) at 200V for 50 minutes. The gels were stained in a solution containing 0.1% (w/v) Coomassie® Brilliant Blue R-250 (VWR chemicals) in 40% (v/v) ethanol and 10% (v/v) acetic acid for 30 minutes and destained in 5% ethanol and 3.5% acetic acid overnight or until the desired background was achieved.

Quantification of resolution improvement

To calculate the resolution improvement of the labelled structures upon expansion, the same cellular areas pre and post expansion were imaged. We calculated the expansion factor by segmenting manually, measuring the nuclear area pre and post expansion in ImageJ and take the square root of this post/pre area ratio. The expected image resolution based on the calculated expansion factor was verified using a line profile across features in the image with expected dimensions of less than 70 nm. A Gaussian curve was fitted to the line profile using the ImageJ FWHM_line macro and these results were used to confirm image resolution. A background subtraction with a rolling ball radius of 50 pixels was performed in ImageJ on the pre-expansion image for the membrane staining before determination of the FWHM.

ASSOCIATED CONTENT

Supporting Information.

The Supporting Information is available free of charge on the ACS Publication website at DOI: .

Scheme S1, The characterization of compounds, Figures S1-S5, Graph S1.

Notes

The authors declare the following competing financial interest(s): V.L., R.K.N. and J.H. are co-founders of Chrometra, a spin-off company, that commercializes the TRITON linkers.

AUTHOR INFORMATION

Corresponding Author

*e-mail correspondence to: johan.hofkens@kuleuven.be

Present Addresses

† School of Chemistry, University of Birmingham, Edgbaston, United Kingdom

§ Chrometra, Kortenaken, Belgium

ORCHID

Aline Acke: 0000-0001-6876-8583

Marisa Vanheusden: 0000-0003-1191-5153

Johan Hofkens: 0000-0002-9101-0567

Author Contributions

‡These authors contributed equally.

V.L., R.K.N. and J.H. designed the research. G.W., M.V., A.A. and D.V. performed the research. M.V., A.A., G.W. and V.L. wrote the article with input from all other authors.

ACKNOWLEDGMENTS

Financial support from the Flemish government through long-term structural funding Methusalem (CASAS2, Meth/15/04) to J.H., from CSC through a fellowship to G.W. (201806210078), from FWO through fellowships to M.V. (1S62318N) and A.A. (1193720N), from KULeuven research fund through ID-N project IDN/19/039 and from EPSRC through grant number EP/Nr020901/1 to R.K.N is gratefully acknowledged. The authors would like to thank R. Nuyts and A. De Weerdt for technical support as well as S. Rocha and W. Vandenberg for the fruitful discussions

REFERENCES

(1) Chen, F.; Tillberg, P. W.; Boyden, E. S. Expansion Microscopy. *Science* **2015**, *347*, 543–548.

(2) Chozinski, T. J.; Halpern, A. R.; Okawa, H.; Kim, H.-J.; Tremel, G. J.; Wong, R. O. L.; Vaughan, J. C. Expansion Microscopy with Conventional Antibodies and Fluorescent Proteins. *Nat. Methods* **2016**, *13*, 485–488.

(3) Ku, T.; Swaney, J.; Park, J.-Y.; Albanese, A.; Murray, E.; Cho, J. H.; Park, Y.-G.; Mangena, V.; Chen, J.; Chung, K. Multiplexed and Scalable Super-Resolution Imaging of Three-

Dimensional Protein Localization in Size-Adjustable Tissues. *Nat. Biotechnol.* **2016**, *34*, 973–981.

(4) Tillberg, P. W.; Chen, F.; Piatkevich, K. D.; Zhao, Y.; Yu, C.-C.; English, B. P.; Gao, L.; Martorell, A.; Suk, H.-J.; Yoshida, F.; et al. Protein-Retention Expansion Microscopy of Cells and Tissues Labeled Using Standard Fluorescent Proteins and Antibodies. *Nat. Biotechnol.* **2016**, *34*, 987–992.

(5) Chen, F.; Wassie, A. T.; Cote, A. J.; Sinha, A.; Alon, S.; Asano, S.; Daugharthy, E. R.; Chang, J.-B.; Marblestone, A.; Church, G. M.; Raj, A.; Boyden, E. S. Nanoscale Imaging of RNA with Expansion Microscopy. *Nat. Methods* **2016**, *13*, 679–684.

(6) Gao, M.; Maraspini, R.; Beutel, O.; Zehtabian, A.; Eickholt, B.; Honigmann, A.; Ewers, H. Expansion Stimulated Emission Depletion Microscopy (ExSTED). *ACS Nano* **2018**, *12*, 4178–4185.

(7) Halpern, A. R.; Alas, G. C. M.; Chozinski, T. J.; Paredez, A. R.; Vaughan, J. C. Hybrid Structured Illumination Expansion Microscopy Reveals Microbial Cytoskeleton Organization. *ACS Nano* **2017**, *11*, 12677–12686.

(8) Truckenbrodt, S.; Maidorn, M.; Crzan, D.; Wildhagen, H.; Kabatas, S.; Rizzoli, S. O. X10 Expansion Microscopy Enables 25-nm Resolution on Conventional Microscopes. *EMBO Rep.* **2018**, *19*, e45836.

(9) Chang, J.-B.; Chen, F.; Yoon, Y.-G.; Jung, E. E.; Babcock, H.; Kang, J. S.; Asano, S.; Suk, H.-J.; Pak, N.; Tillberg, P. W.; Asmamaw, T. W.; Cai, D.; Boyden, E. S. Iterative Expansion Microscopy. *Nat. Methods* **2017**, *14*, 593–599.

(10) Sheard, T. M. D.; Hurley, M. E.; Colyer, J.; White, E.; Norman, R.; Pervolaraki, E.; Narayanasamy, K. K.; Hou, Y.; Kirton, H. M.; Yang, Z.; Hunter, L.; Shim, J. U.; Clowsley,

A. H.; Smith, A. J.; Baddeley, D., Soeller, C. Colman, M. A.; Jayasinghe, I. Three-Dimensional and Chemical Mapping of Intracellular Signaling Nanodomains in Health and Disease with Enhanced Expansion Microscopy. *ACS Nano* **2019**, *13*, 2143–2157.

(11) Legant, W. R.; Shao, L.; Grimm, J. B.; Brown, T. A.; Milkie, D. E.; Avants, B. B.; Lavis, L. D.; Betzig, E. High-Density Three-Dimensional Localization Microscopy across Large Volumes. *Nat. Methods* **2016**, *13*, 359–365.

(12) Abd-El-Basset, E. M.; Fedoroff, S. Contractile Units in Stress Fibers of Fetal Human Astroglia in Tissue Culture. *J. Chem. Neuroanat.* **1994**, *7*, 113–122.

(13) Fischer, M.; Kaech, S.; Knutti, D.; Matus, A. Rapid Actin-Based Plasticity in Dendritic Spines. *Neuron* **1998**, *20*, 847–854.

(14) Gambarotto, D.; Zwettler, F. U.; Guennec, M. L.; Schmidt-Cernohorska, M.; Fortun, D.; Borgers, S.; Heine, J.; Schloetel, J.-G.; Reuss, M.; Unser, M.; Boyden, E. S.; Sauer, M.; Hamel, V.; Guichard, P. Imaging Cellular Ultrastructures Using Expansion Microscopy (U-ExM). *Nat. Methods* 2019, 16, 71-74.

(15) Li, R.; Chen, X.; Lin, Z.; Wang, Y.; Sun, Y. Expansion Enhanced Nanoscopy. *Nanoscale* **2018**, *10*, 17552–17556.

(16) Wang, Y.; Yu, Z.; Cahoon, C. K.; Parmely, T.; Thomas, N.; Unruh, J. R.; Slaughter, B. D.; Hawley, R. S. Combined Expansion Microscopy with Structured Illumination Microscopy for Analyzing Protein Complexes. *Nat. Protoc.* **2018**, *13*, 1869-1895.

(17) Park, Y.-G.; Sohn, C. H.; Chen, R.; McCue, M.; Yun, D. H.; Drummond, G. T.; Ku, T.; Evans, N. B.; Oak, H. C.; Trieu, W.; Choi, H.; Jin, X.; Lilascharoen, V.; Wang, J.; Truttman, M. C.; Qi, H. W.; Ploegh, H. L.; Golub, T. R.; Chen, S.-C.; Frosch, M. P.; et al. Protection

of Tissue Physicochemical Properties Using Polyfunctional Crosslinkers. *Nat. Biotechnol.* **2019**, *37*, 73–83.

(18) Truckenbrodt, S.; Sommer, C.; Rizzoli, S. O.; Danzl, J. G. A Practical Guide to Optimization in X10 Expansion Microscopy. *Nat. Protoc.* **2019**, *14*, 832.

(19) Asano, S. M.; Gao, R.; Wassie, A. T.; Tillberg, P. W.; Chen, F.; Boyden, E. S. Expansion Microscopy: Protocols for Imaging Proteins and RNA in Cells and Tissues. *Curr. Protoc. Cell Biol.* **2018**, *80*, e56.

(20) Fujimoto, T.; Parmryd, I. Interleaflet Coupling, Pinning, and Leaflet Asymmetry-Major Players in Plasma Membrane Nanodomain Formation. *Front. Cell Dev. Biol.* **2017**, *4*, 155–155.

(21) Shim, S.-H.; Xia, C.; Zhong, G.; Babcock, H. P.; Vaughan, J. C.; Huang, B.; Wang, X.; Xu, C.; Bi, G.-Q.; Zhuang, X. Super-Resolution Fluorescence Imaging of Organelles in Live Cells with Photoswitchable Membrane Probes. *Proc. Natl. Acad. Sci. U. S. A.* **2012**, *109*, 13978–13983.

(22) Bian, X.; Xiao, Y.-T.; Wu, T.; Yao, M.; Du, L.; Ren, S.; Wang, J. Microvesicles and Chemokines in Tumor Microenvironment: Mediators of Intercellular Communications in Tumor Progression. *Mol. Cancer* **2019**, *18*, 50.

(23) Muralidharan-Chari, V.; Clancy, J. W.; Sedgwick, A.; D'Souza-Schorey, C. Microvesicles: Mediators of Extracellular Communication during Cancer Progression. *J. Cell Sci.* **2010**, *123*, 1603–1611.

(24) Revelo, N. H.; Kamin, D.; Truckenbrodt, S.; Wong, A. B.; Reuter-Jessen, K.; Reisinger, E.; Moser, T.; Rizzoli, S. O. A New Probe for Super-Resolution Imaging of Membranes Elucidates Trafficking Pathways. *J. Cell Biol.* **2014**, *205*, 591–606.

(25) Shi, X.; Li, Q.; Dai, Z.; Tran, A.; Feng, S.; Ramirez, A. D.; Lin, Z.; Wang, X.; Chow, T. T.; Seiple, I. B.; Huang, B. Label-Retention Expansion Microscopy. *bioRxiv* **2019**, 687954. DOI: 10.1101/687954.

For Table of Contents only

